Laser emission in a mesastructure with HgCdTe-based quantum wells with a periodic ridge system

© E.N. Kiryanova[1,2], V.V. Rumyantsev[1,2], A.A. Razova[1,2,¶], D.V. Shengurov[1], N.S. Gusev[1], E.E. Morozova[1], V.V. Utochkin[1], V.R. Baryshev[3], A.A. Yantser[1], K.A. Mazhukina[1], M.A. Fadeev[1], N.S. Ginzburg[3], A.M. Malkin[3], E.D. Egorova[3], N.N. Mikhailov[4], S.A. Dvoretsky[4], V.I. Gavrilenko[1,2], S.V. Morozov[1,2]

[1] Institute for Physics of Microstructures of Russian Academy of Sciences, 603950 Nizhny Novgorod, Russia
[2] Lobachevsky State University, 603950 Nizhny Novgorod, Russia
[3] Gaponov-Grekhov Institute of Applied Physics of the Russian Academy of Sciences, 603950 Nizhny Novgorod, Russia
[4] Institute of Semiconductor Physics, Siberian Branch of Russian Academy of Sciences, 630090 Novosibirsk, Russia

E-mail: annara@ipmras.ru

Received October 15, 2025
Revised December 3, 2025
Accepted December 5, 2025

In a waveguide structure with HgCdTe quantum wells single-frequency laser emission at a wavelength of 13.5 μm is demonstrate due to the formation of a periodic system of ridges on the surface of the structure, implementing distributed feedback. It is shown that the ion etching technology used does not lead to an increase in the threshold intensity of optical pumping, which does not exceed 100 W/cm^2 at $T < 20$ K.

Keywords: HgCdTe, mesastructures, distributed feedback, single-frequency laser.

DOI: 10.61011/SC.2025.10.62869.8664

1. Introduction

The development of absorption spectroscopy techniques for various gases and organic compounds in the mid- and far-infrared (IR) ranges is important both for fundamental research and for current applications [1]. Solving such problems requires, in particular, the creation of compact semiconductor coherent radiation sources with high temperature and frequency stability, good output power and low generation thresholds. The undisputed leaders here are quantum cascade lasers (QCL) based on semiconductors $\mathrm{A^{III}B^{V}}$ [2,3], however, the region of 25$-$60 μm remains inaccessible to them due to strong phonon absorption in these materials [3]. It is in this range that interband lasers based on narrow-band materials could compete with QCL, in which the band of residual rays is located in a lower frequency range compared to $\mathrm{A^{III}B^{V}}$ — first of all, these are compounds of lead-tin chalcogenides PbSnSe(Te) and cadmium–mercury–tellurium HgCdTe [4]. A critically important feature of the band spectrum in these materials is the hyperbolic law of carrier dispersion [5,6], which contributes to the suppression of nonradiative Auger processes. In relation to PbSnTe and PbSnSe, such a dispersion of electrons and holes is realized in bulk films, and laser generation at wavelengths of 20$-$50 μm with current pumping has been demonstrated in them at cryogenic temperatures [7]. At the same time, the development of PbSnSe(Te)lasers is hindered by a significant misalignment of the lattices in this heterosystem and, consequently, by the high defectiveness of the resulting structures. As for HgCdTe, it is a well-coordinated heterosystem with the highest crystalline perfection of the formed layers, indispensable in photodetector applications [5]. The hyperbolic dispersion law required to suppress Auger recombination is not implemented in bulk HgCdTe, but can be obtained in quantum wells (QWs) of HgCdTe/CdHgTe (in the vicinity of Γ-dot $k_{\parallel} = 0$) [8], and such QWs have long been proposed in theoretical works (for example, in Refs. [9,10]) as an active medium for long-wavelength lasers.

The experimental component of the work on ultra-long-wavelength HgCdTe lasers has been acquired quite recently [8]: stimulated emission (SE) at wavelengths from 25 to 31 μm (which goes beyond the capabilities of existing QCL) in the temperature range of 8$-$90 K has been demonstrated in heterostructures with HgTe/CdHgTe QWs for optical pumping. One of the important areas of development of these works is the search for optimal implementations of instrument (laser) structures that are convenient in terms of both their formation technology and output characteristics in terms of power, generation thresholds, and radiation directivity. In particular, microdisc resonators were implemented here and laser emission (LE) was obtained at wavelengths near 25 μm [11]. However, generation in microdisks was achieved at temperatures noticeably lower than the maximum observation temperature of SE in non-processed structures, and the generation threshold significantly exceeded the thresholds for the occurrence of SE. This was associated in Ref. [11] with defect formation (and the appearance of a large number of nonradiative recombination centers) during the processing of microdisc resonators, which includes magnetron sputtering of a metal mask and ion etching (IE) to a depth of $> 4\,\mu$m. In addition, the problem is the directional output of radiation from microdisc lasers, and the question remains of optimal resonator designs that would make it possible to obtain long-wavelength laser generation with low thresholds during optical pumping over a wide temperature range in heterostructures with HgCdTe QW.

The purpose of this paper is to develop this approach based on a model heterostructure with a HgCdTe/CdHgTe core emitting at a wavelength of $\sim 14\,\mu$m, to create a distributed feedback laser (DFB) based on heterostructures with a HgCdTe/CdHgTe core in the long wavelength ($> 29\,\mu$m) of the mid-IR range, inaccessible to modern QCL.

A DFB laser structure with a periodic ridge system is formed in this study based on a waveguide heterostructure with HgCdTe/CdHgTe QW, and single-frequency laser generation is shown in it. A similar DFB laser is actually a one-dimensional photonic crystal of macroscopic size, which is more resistant (compared, for example, with relatively narrow strip resonators) to random defects on the surface of the structure, and also allows for high Q-factor with relatively shallow etching of the structure. A deliberately successful model HgCdTe heterostructure was chosen as the initial model, emitting at a wavelength of $\sim 14\,\mu$m and demonstrating stimulated emission in case of both pulsed and continuous pumping. At the same time, the approaches developed in the study can also be used to create HgCdTe/CdHgTe DFB lasers based on heterostructures in the long-wavelength ($> 29\,\mu$m) part of the mid-IR range, inaccessible to modern lasers.

2. Materials and research methods

$Hg_{1-x}Cd_xTe/Cd_yHg_{1-y}Te$ waveguide heterostructure with QWs grown by molecular beam epitaxy (MBE) on a substrate *i*-GaAs (013) was studied in this paper. The thickness of the buffer layer (D_{buf}) CdTe is $10\,\mu$m. The CdHgTe waveguide layer located on top of the buffer provides localization of the TE_0-mode of the interband radiation in the QW region due to a higher refractive index compared to the buffer layer. The thickness of the lower waveguide layer (adjacent to the CdTe buffer) is $D_1 = 1.9\,\mu$m, the thickness of the active region is $D_{\text{act}} = 0.3\,\mu$m, and the thickness of the upper waveguide layer is $D_2 = 3\,\mu$m. The structure was covered with a CdTe protective layer of with a thickness of 50 nm. The active region contained $N_{QW} = 5$ QW with a thickness of $d_{QW} = 7.4$ nm and Cd content in QW of $x = 9.8\,\%$, and in barrier/waveguide layers $y = 69\,\%$ [12] (Figure 1, *a*).

The formation of a mesastructure with a one-dimensional photonic crystal was performed by IE using laser lithography. Etching was carried out with argon ions with an energy of ~ 1.4 keV in previously tested modes of manufacturing of mesastructures based on heterostructures with HgCdTe

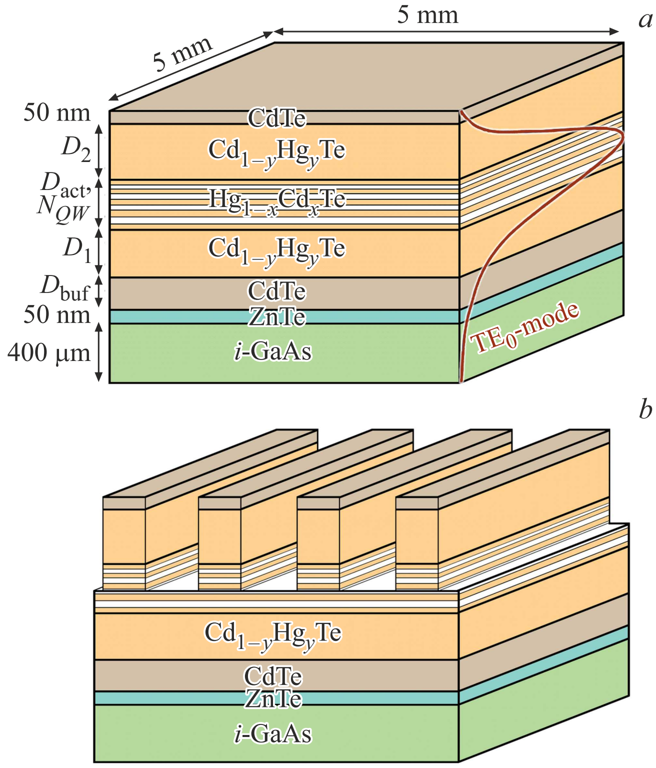

Figure 1. Diagrams of the initial structure (*a*) and mesastructure with ridges (*b*).

QW [11]. The design of the ridge was calculated based on the assumption that the etching depth did not exceed the depth of the QW and was $2\,\mu$m, however, the resulting height of the ridges was $3.2\,\mu$m, which leads to partial etching of the active area between the ridges (Figure 1, *b*). According to the scanning electron microscope (SEM) images, the distance between the ridges varies from 3.55 to $3.65\,\mu$m, and the width of the ridge varies from 2.79 to $3.94\,\mu$m. The length of the lattice along the ridges is 2 mm and 1 cm in the orthogonal direction (Figure 2).

Microscopic characterization of structures was carried out using methods (SEM). The photoluminescence (PL) and SE spectra were recorded using a Bruker Vertex 80v Fourier spectrometer in step-by-step scanning mode. An HgCdTe-based photodetector with a red boundary of $16\,\mu$m was used to register the signal. A diode laser with a wavelength of 808 nm was used as a pump to measure the PL spectra. A CO_2 laser with a wavelength of $\lambda = 10.6\,\mu$m and a radiation intensity of up to $\sim 200\,\text{kW/cm}^2$ was used for optical excitation in SE studies. The pulse duration of the CO_2-laser is 100 ns at a repetition rate of 33 Hz.

3. Results

Figure 3 shows the PL and SE spectra for the initial structure, as well as the emission spectrum of the formed laser mesastructure. The SE and LE spectra were identified

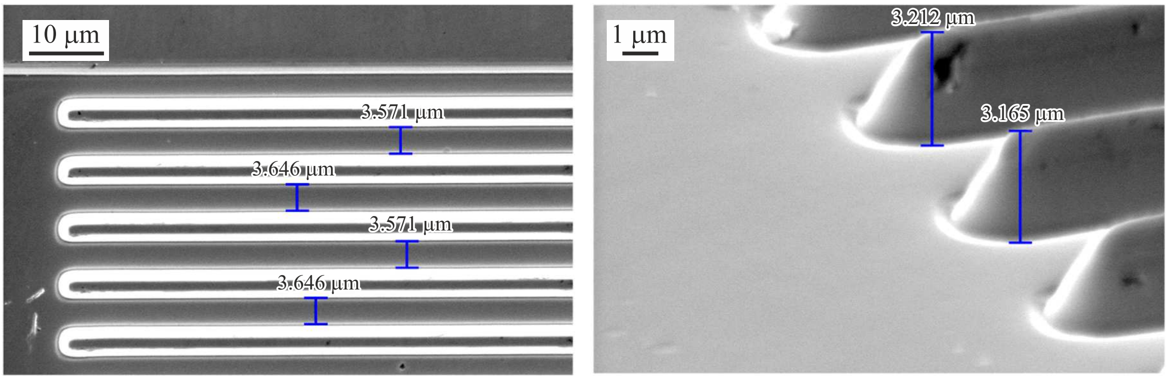

Figure 2. SEM images of a mesastructure with a DFB on a periodic system of etched ridges (left — top view, right — side view).

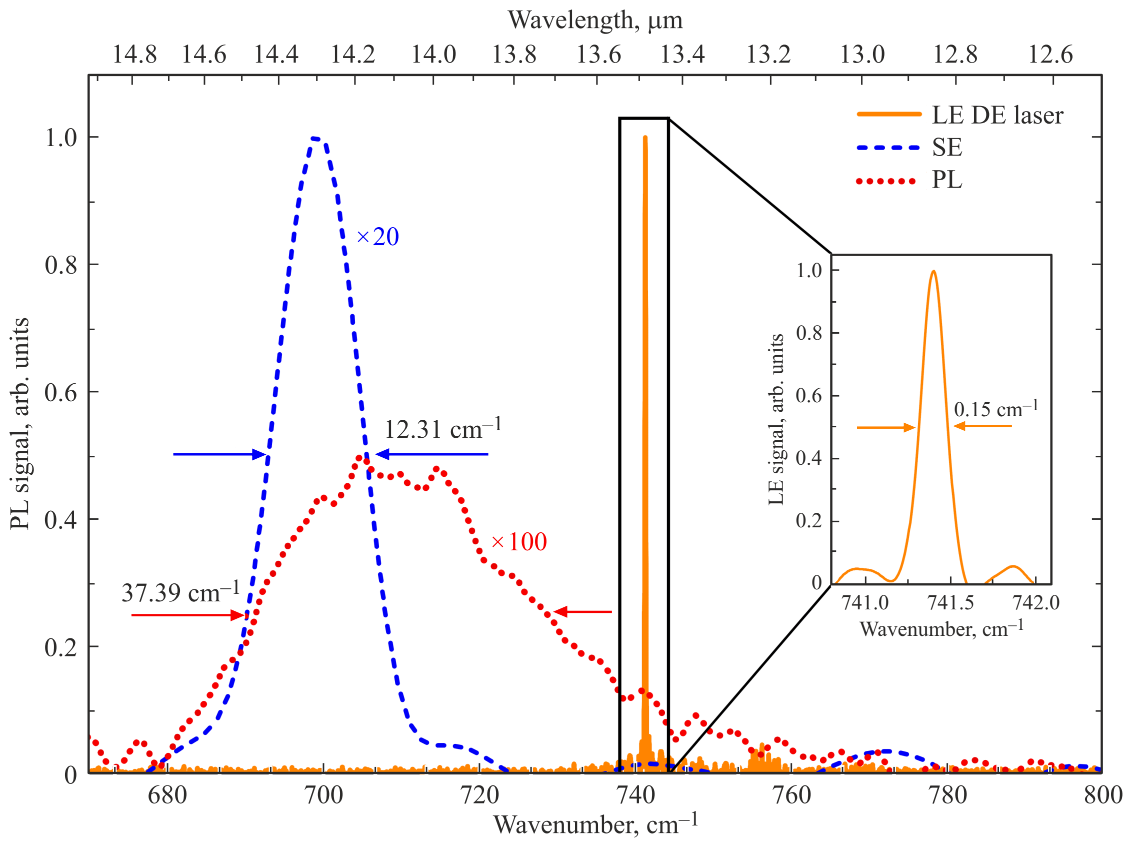

Figure 3. Spectra: blue dotted curve — stimulated emission (SE) of an unprocessed sample, red dots — photoluminescence (PL) of an unprocessed sample [13], orange curve — laser emission of a „DFB laser" (LE DF laser). The values by which the signal intensities were multiplied are indicated next to the spectra.

by decreasing the spectral line width and the „threshold" (superlinear) increase in the integral emission power of the sample from the pumping power. It should be noted that the width of the half-height radiation spectrum for an unprocessed sample under pulsed excitation is $\sim 12\,\mathrm{cm}^{-1}$, i.e., 3 times greater than $0.7k_BT = 3.89\,\mathrm{cm}^{-1}$, where k_B is the Boltzmann constant, T is the temperature. However, the narrowing of the radiation line compared to the PL line (Figure 3) and the dependence of the emission power of the sample on the pumping power in the pulsed mode allow us to conclude that the radiation is stimulated.

For the „DFB laser" the line width at half height is $0.15\,\mathrm{cm}^{-1}$, i.e. 26 times less than the value of $7k_BT = 3.89\,\mathrm{cm}^{-1}$, which clearly indicates that the radiation line cannot be associated with spontaneous optical transitions. In addition, a narrowing of the spectrum by more than an order of magnitude compared to the SE line indicates a sharp increase in the Q-factor of the emitting

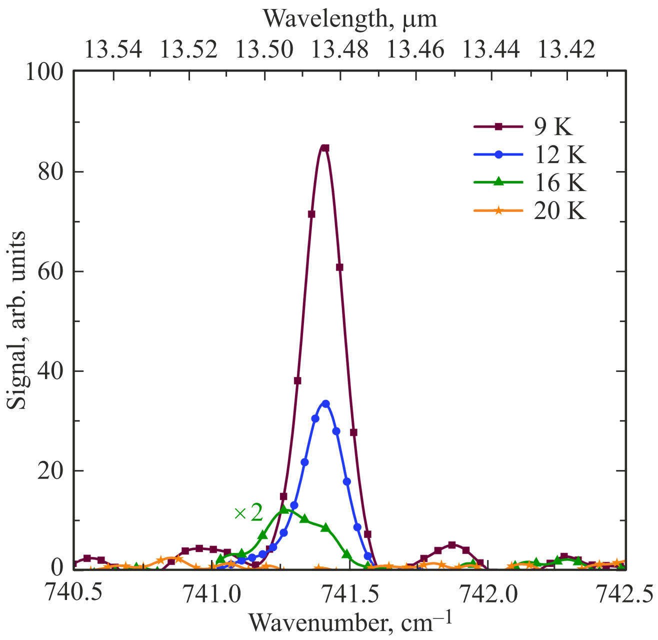

Figure 4. The temperature dependence of the LE obtained for the „DFB laser" in case of pumping by CO_2-laser with an intensity of 154 W/cm^2.

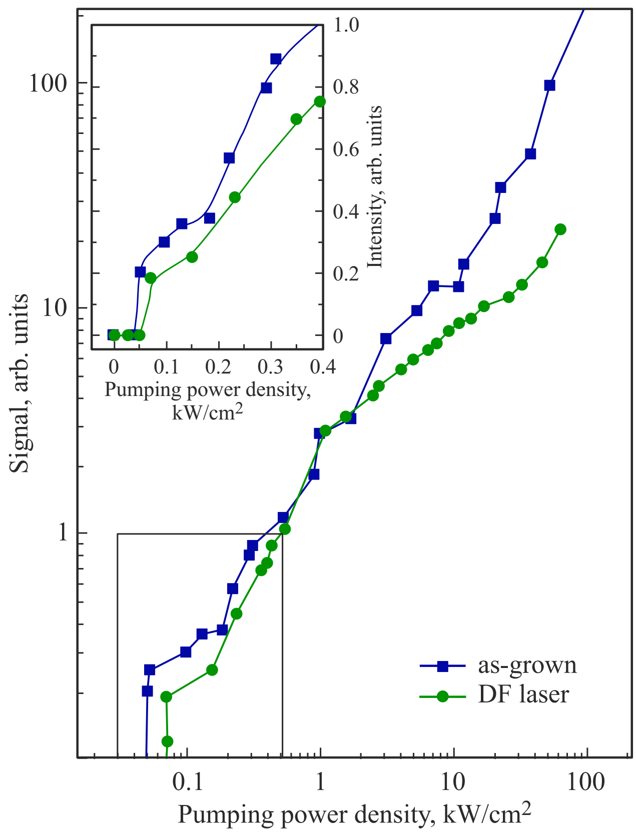

Figure 5. Dependence of the emission intensity on the power density of the pumping laser at $T = 8$ K on a logarithmic scale: blue squares — unprocessed structure (as-grown), green circles — mesastructures with a DFB (DF laser). The brown rectangle indicates the area shown in the insert on a linear scale.

system due to the presence of strong positive feedback at the observed generation wavelength.

It can be seen that the SE peak, characteristic of the unprocessed structure, corresponds to a wave number of 700 cm^{-1} (or a wavelength of 14.3 μm), while the peak radiation of the „DFB laser" corresponds to the wave number 741.3 cm^{-1} (13.5 μm). In our type of „DFB laser" it is necessary to fulfill the Bragg resonance condition, which, as is known, is given by the equality [14,15]

$$\lambda_{Br} = 2n_{\text{eff}}d/s,$$

where n_{eff} is the effective refractive index, d is the grating period, s is the harmonic number. As can be seen from the spectrum of the interband PL (Figure 3, red dots) from QWs located in the active region of the waveguide structure, the gain spectrum corresponds to wavenumbers from 680 to 760 cm^{-1}, which includes the frequency of the Bragg resonance for this lattice at the third harmonic. Since in the studied structure $d = 7 \pm 0.2\,\mu$m, and the position of the radiation line at the third harmonic corresponds to 13.5 μm, then $n_{\text{eff}} = 2.89 \pm 0.05$, which coincides with the characteristic value of the effective refractive index for CdHgTe. Thus, the peak radiation of the „DFB laser" is „fixed" by the electrodynamic properties of the selected DFB design, and is not determined by the maximum in the gain spectrum, as in the case of SE. The fixation of the radiation wavelength is also clearly seen in the dependence of the radiation spectra on temperature (Figure 4). As the temperature increases, the SE line shifts towards higher quantum energies due to an increase in the band gap (E_g), while the position of the line practically does not change in the structure with DFB. However, an increase in E_g determines the maximum generation temperature of the „DFB laser", since with an increase in temperature E_g there is more quantum energy at which generation in this type of DFB is possible.

Figure 5 shows the dependences of the radiation power of the unprocessed structure and the formed mesastructure with a growth. It can be seen that the dependences coincide with good accuracy at the pumping intensity $I_p < 2$ kW/cm^2, decreasing linearly. A sharp drop (by an order of magnitude) of the detector signal is observed in the region of $I_p < 100$ W/cm^2 for both structures to the noise level, identified with the generation threshold. For an unprocessed structure, the threshold pumping intensity was 50 ± 10 W/cm^2, and for a mesastructure with a growth of $\sim 70 \pm 15$ W/cm^2, while for other types of resonators the increase in the generation threshold for processed structures was at least one order of magnitude [11].

4. Conclusion

Thus, single-frequency laser emission in HgCdTe-based laser structures with DFB is demonstrated in this paper. Within the limits of measurement error, the generation threshold for the mesastructure with DFB has not changed compared to the initial structure, which allows us to conclude that there are no additional recombination defects in the QW introduced by post-layer processing technology. The latter determines the prospects of the approach used to create HgCdTe-based lasers in the longer wavelength region, where recombination through defects plays a particularly important role [12].

Funding

The growth of structures, the formation of a DFB laser, and the study of the optical properties of mesastructures using PL and SE spectra were carried out with the financial support of the Russian Science Foundation (grant No. 22-12-00310-P). The characterization of structures performed with the help of SEM was carried out within the framework of the state assignment of the IAP RAS (project No. FFUF-2024-0019).

Conflict of interest

The authors declare that they have no conflict of interest.

References

[1] M. Lamperti, R. Gotti, D. Gatti, M.K. Shakfa, E. Can, F. Tamassia, P. Schunemann, P. Laporta, A. Farooq, M. Marangoni. Commun. Phys., **3** (1), 175 (2020). DOI: https://doi.org/10.1038/s42005-020-00441-y

[2] M. Razeghi, N. Bandyopadhyay, Y. Bai, Q. Lu, S. Slivken. Opt. Mater. Express, **3** (11), 1872 (2013). DOI: https://doi.org/10.1364/OME.3.001872

[3] M.S. Vitiello, G. Scalari, B. Williams, P. De Natale. Opt. Express, **23** (4), 5167 (2015). DOI: https://doi.org/10.1364/OE.23.005167

[4] D.N. Talwar, M. Vandevyver. J. Appl. Phys., **56** (6), 1601 (1984). DOI: http://dx.doi.org/10.1063/1.334144

[5] A. Rogalski, M. Kopytko, W. Hu, P. Martyniuk. Sensors, **23**, 7564 (2023). DOI: https://doi.org/10.3390/s23177564

[6] J.O. Dimmock, I. Melngailis, A.J. Strauss. Phys. Rev. Lett., **16** (26), 1193 (1966). DOI: https://doi.org/10.1103%2FPhysRevLett.16.1193

[7] K.V. Maremyanin, A.V. Ikonnikov, L.S. Bovkun, V.V. Rumyantsev, E.G. Chizhevsky, I.I. Zasavitsky, V.I. Gavrilenko. FTP, **52** (12), 1486 (2018). (in Russian). DOI: https://doi.org/10.21883/FTP.2018.12.46762.42

[8] S.V. Morozov, V.V. Rumyantsev, M.S. Zholudev, A.A. Dubinov, V.Ya. Aleshkin, V.V. Utochkin, M.A. Fadeev, K.E. Kudryavtsev, N.N. Mikhailov, S.A. Dvoretskii, V.I. Gavrilenko, F. Teppe. ACS Photonics, **8** (12), 3526 (2021). DOI: https://doi.org/10.1021/acsphotonics.1c01111

[9] V.M. Menon, L.R. Ram-Mohan, I. Vurgaftman, J.R. Meyer. J. Electron. Mater., **29** (6), 865 (2000). DOI: https://doi.org/10.1007/s11664-000-0239-5

[10] A.A. Dubinov, V.Y. Aleshkin, V.V. Rumyantsev, S.V. Morozov. Optical Quant. Electron., **57** (6), 369 (2025). DOI: https://doi.org/10.1007/s11082-025-08291-0

[11] A.A. Razova, V.V. Rumyantsev, K.A. Mazhukina, V.V. Utochkin, M.A. Fadeev, A.A. Dubinov, V.Ya. Aleshkin, N.N. Mikhailov, S.A. Dvoretsky, D.V. Shengurov, N.S. Gusev, E.E. Morozova, V.I. Gavrilenko, S.V. Morozov. Appl. Phys. Lett., **126** (12), 121102 (2025). DOI: https://doi.org/10.1063/5.0253661

[12] V.V. Rumyantsev, K.A. Mazhukina, V.V. Utochkin, K.E. Kudryavtsev, A.A. Dubinov, V.Ya. Aleshkin, A.A. Razova, D.I. Kuritsin, M.A. Fadeev, A.V. Antonov, N.N. Mikhailov, S.A. Dvoretsky, V.I. Gavrilenko, F. Teppe, S.V. Morozov. Appl. Phys. Lett., **124** (16), 161111 (2024). DOI: https://doi.org/10.1063/5.0186292

[13] V. Rumyantsev, M. Fadeev, V. Aleshkin, N. Kulikov, V. Utochkin, N. Mikhailov, S. Dvoretskii, S. Pavlov, H.-W. Hübers, V. Gavrilenko, C. Sirtori, Z.F. Krasilnik, S. Morozov. Phys. Status Solidi B, **256** (6), 1800546 (2019). DOI: https://doi.org/10.1002/pssb.201800546

[14] H. Kogelnik. *Integrated optics* (Berlin–Heidelberg, Springer, 1975). 2. *Theory of dielectric waveguides*, pp. 13–81. DOI: https://doi.org/10.1007/BFb0103618

[15] V.R. Baryshev, E.D. Egorova, N.S. Ginzburg, E.R. Kocharovskaya, A.M. Malkin, V.Yu. Zaslavsky, S.V. Morozov, A.C. Sergeev. FTP, **57** (5), 362 (2023). (in Russian). DOI: https://doi.org/10.21883/FTP.2023.05.56204.41k

Translated by A.Akhtyamov